

# Preliminary numerical analysis of controllable prestressed wale system for deep excavation

Chang Il Lee<sup>1</sup>, Eun Kyum Kim<sup>1</sup>, Jong Sik Park<sup>2</sup> and Yong-Joo Lee<sup>\*1</sup>

<sup>1</sup>Department of Civil Engineering, Seoul National University of Science and Technology,  
232 Gongneung-ro, Nowon-gu, Seoul 01811, Republic of Korea

<sup>2</sup>Civil Business Team, TAEYOUNG E&C, 111 Yeouigongwon-ro, Yeongdeungpo-gu, Seoul 07241, Republic of Korea

(Received November 13, 2017, Revised January 25, 2018, Accepted January 30, 2018)

**Abstract.** The main purpose of retaining wall methods for deep excavation is to keep the construction site safe from the earth pressure acting on the backfill during the construction period. Currently used retaining wall methods include the common strut method, anchor method, slurry wall method, and raker method. However, these methods have drawbacks such as reduced workspace and intrusion into private property, and thus, efforts are being made to improve them. The most advanced retaining wall method is the prestressed wale system, so far, in which a load corresponding to the earth pressure is applied to the wale by using the tension of a prestressed (PS) strand wire. This system affords advantages such as providing sufficient workspace by lengthening the strut interval and minimizing intrusion into private properties adjacent to the site. However, this system cannot control the tension of the PS strand wire, and thus, it cannot actively cope with changes in the earth pressure due to excavation. This study conducts a preliminary numerical analysis of the field applicability of the controllable prestressed wale system (CPWS) which can adjust the tension of the PS strand wire. For the analysis, back analysis was conducted through two-dimensional (2D) and three-dimensional (3D) numerical analyses based on the field measurement data of the typical strut method, and then, the field applicability of CPWS was examined by comparing the lateral deflection of the wall and adjacent ground surface settlements under the same conditions. In addition, the displacement and settlement of the wall were predicted through numerical analysis while the prestress force of CPWS was varied, and the structural stability was analysed through load tests on model specimens.

**Keywords:** retaining wall methods, controllable prestressed wale system (CPWS), finite element analysis, indoor model test

## 1. Introduction

Deep excavations in urban areas must be performed in consideration of factors such as land expropriation, influence of adjacent structures, and changes in groundwater level. The size and depth of such excavations are gradually increasing owing to the demands of users and contractors. Therefore, many studies have developed methods for ensuring stability against excavation and supporting the earth pressure acting on the workspace (Lee *et al.* 1998, Onishi and Sugawara 1999, Long 2001, Leung *et al.* 2009, Usmani *et al.* 2010, Osman and Bolton 2007, Ou *et al.* 2000, Huang *et al.* 2012, Xu *et al.* 2013, Dang *et al.* 2012, Chowdhury *et al.* 2013, Dong 2014, Dong *et al.* 2016, Osman and Bolton 2006, Pickels *et al.* 2003, Kung 2010, Usluogullari *et al.* 2015, Li *et al.* 2015). The slurry wall method, strut method, and prestressed wale system are commonly used to support retaining walls in deep excavation. The anchor system is designed to resist the earth pressure transmitted to the wall of the excavation surface through the resistance obtained from the tension of

a prestressed (PS) strand wire. If there is a large difference between the elevation of the excavation section or the bottom surface, this system affords an advantage in that there is no restriction on the use of construction machines. However, if the anchor is too long, it may intrude on the construction boundary.

The strut method is the most common retaining wall method. In this method, a wall is installed at the excavation boundary, and this wall is supported using struts and wales. Although this method is mechanically safe and economical, it is difficult to realize sufficient workspace, and the potential buckling of struts poses a risk in the case of deep excavations.

Prestressed wale systems have been developed and widely used for overcoming the abovementioned shortcomings of excavation methods (Park *et al.* 2009, Park *et al.* 2004, Kim *et al.* 2004, Kim *et al.* 2005a, Kim *et al.* 2005b, Kim *et al.* 2007). However, the drawback of prestressed wale systems is that they cannot adjust the tension of the PS strand wire for the wale that is required to resist the earth pressure transmitted from the back to the wall.

In this study, back analysis was conducted based on measurements of a site where the strut method was applied, and numerical analysis was conducted for applying the controllable prestressed wale system (CPWS) to the same

---

\*Corresponding author, Professor  
E-mail: [ucesyjl@seoultech.ac.kr](mailto:ucesyjl@seoultech.ac.kr)

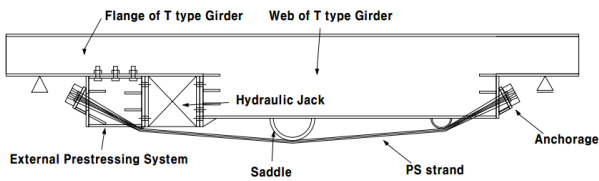


Fig. 1 Composition of CPWS

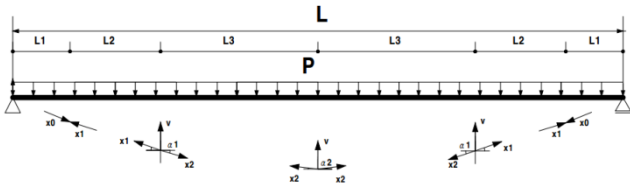


Fig. 2 Free body diagram of CPWS

ground conditions. The CPWS numerical analysis was conducted while the horizontal force acting on the wall was varied, and the strut method, wall horizontal displacement, and ground surface settlement were analysed. In addition, the structural stability of the CPWS and the system safety owing to variations in the tension of the PS strand wire were investigated through indoor model tests.

**2. Controllable prestressed wale system (CPWS)**

Existing retaining wall strut methods suffer from problems such as constructability degradation owing to increased steel material usage, wall displacement and earth pressure uncertainties, and increased construction cost. CPWS introduces prestress to overcome these problems, and it can adjust the prestress according to the wall deformation owing to the earth pressure. Therefore, CPWS can improve the constructability, stability, and economic efficiency because it enables efficient use of the workspace through a long-span support.

*2.1 Concept of CPWS*

Fig. 1 shows the main components of CPWS. The T-type girder cross section includes a wide flange on the sides and a web with a large cross section in the centre. This cross-section configuration considers the effect of the bending moment redistribution. The bending moment owing to earth pressure is offset by the prestress force, and the bending stress and deflection are reduced by the large cross section in the centre. When a long span is applied to the strut interval, the bending moment and deflection in the centre increase owing to the earth pressure. Therefore, prestress is introduced to offset the stress and displacement. In addition, the eccentricity is increased by arranging the PS strand wire in a curve by using the T-type girder and saddle to avoid the excessive use of the PS strand wire and PS force. The PS strand wire is fixed at both ends of the T-type girder, and an external prestressing system and a hydraulic jack are installed at an end so that the PS force can be adjusted to an appropriate moment according to the change in the earth pressure.

Fig. 2 shows a free body diagram of CPWS. The tension

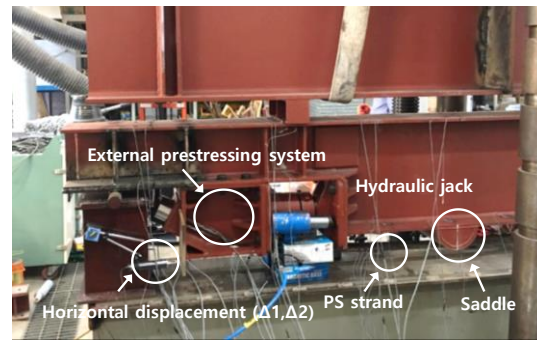


Fig. 3 Laboratory model test for CPWS

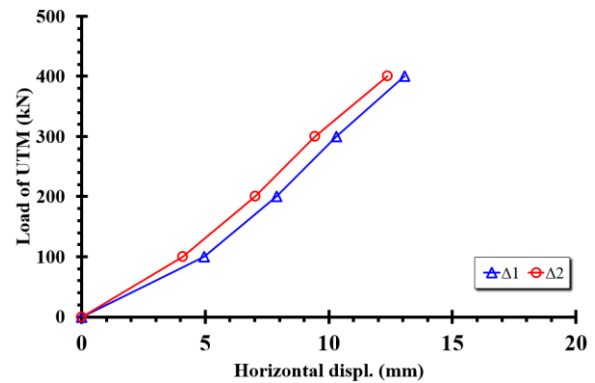


Fig. 4 Horizontal displacement of external prestressing system by prestressing force

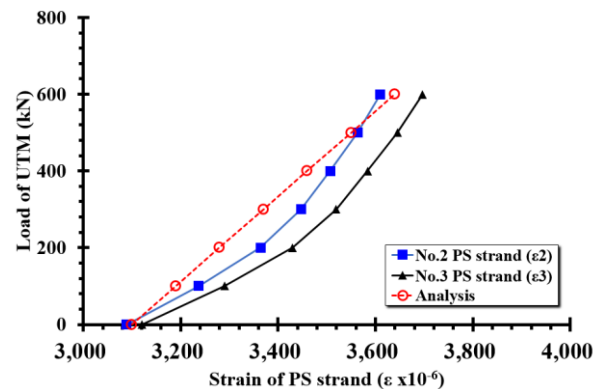


Fig. 5 Variation of prestressing force by increase in UTM load

of the PS strand wire is transmitted to the T-type girder through five nodes, and the T type girder serves to offset the earth pressure acting on the wall. In other words, the PS forces  $x_1$  and  $x_2$  introduced by the PS strand wire generate

force  $V$  in the vertical direction to the T-type girder in the saddle and fixing devices, and this force offsets the earth pressure acting on the T-type girder.

## 2.2 Laboratory model test

To investigate the field applicability of CPWS, load tests for simulating the earth pressure were conducted in a laboratory. Fig. 3 shows the load test system and measurement situation constructed for this purpose. The earth pressure delivered from the back of the retaining wall was simulated using a universal test machine (UTM), and the tension of the PS strand wire was adjusted according to the increase or decrease in earth pressure.

Fig. 4 shows the horizontal displacement when a 400-kN PS force was applied to the T-type girder shown in Fig. 1. The horizontal displacement was measured as 12.730 mm/400kN and 7.465mm/200kN; this is equaled to 0.0263 mm/kN when converted to the unit PS force ([12.730-7.465]mm/[400-200]kN). In addition, the horizontal displacement according to the elastic analysis was 0.02503 mm/kN; this was similar to the measured value of 0.0263 mm/kN.

Fig. 5 shows the measured strain values by the position in the PS strand wire when stepwise load was applied to the T-type girder with the introduction of a 400-kN PS force. As the earth pressure increases on the T-type girder, the PS strand wire length and PS force increase by  $\Delta S$  and  $\Delta X$ . These values are interpreted by applying the three equilibrium equations as well as the compatibility condition that the sum of the horizontal displacement caused by the earth pressure and the displacement caused by the PS force is 0. The analysis result showed that when a 400-kN load was applied, the PS force increase in the PS strand wire was 43.0 kN. When a 600-kN load was applied, the PS force increase in the PS strand wire was 60.9 kN. When this was converted based on a 400-kN load, the measured PS force increase was 40.6 kN; this is in good agreement with the analytical value of 43.0 kN.

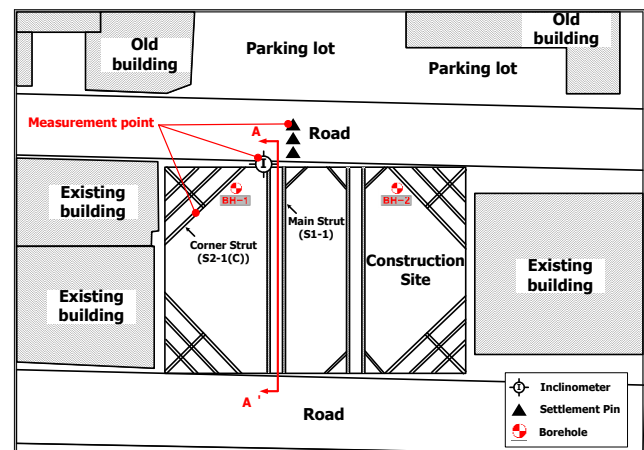
From the above results, the horizontal displacement of the PS force by the analysis and the PS force increase by the applied load tend to agree with the measurement results. When analysis equations that consider the equilibrium conditions and deformation compatibility condition shown in Fig. 4 are applied, it will be possible to predict the varying earth pressure. In this study, laboratory model tests were conducted using a load application device. The results showed that CPWS could easily respond to the earth pressure variation through the T-type girder and adjust the PS force accordingly. Despite such force adjustment, its structural stability was ensured.

## 3. Field application

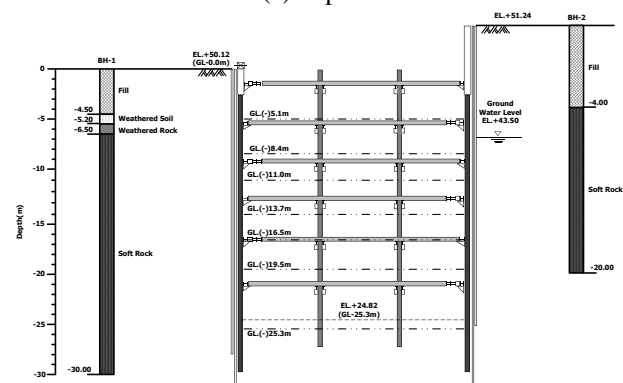
To analyse the field applicability of CPWS through numerical analysis, back analysis was conducted based on the measurement data of a site that used the existing strut method. CPWS was numerically analysed and compared with the existing strut method. In addition, the results were compared while varying the PS force.



Fig. 4 Construction site



(a) Top view



(b) Cross section of A-A'

Fig. 5 View of construction site

### 3.1 Construction site and ground condition

The construction site that used the existing strut method was a new building with 11 ground floors and 4 underground floors located in Nonhyeon-dong, Seoul (Fig. 4). Excavation was performed up to a depth of 25.0 m from

Table 1 Construction phase

Stages	Period: dates	Interval days	Construction activities
1	2016.06.01-07.15	52	Lining, side pile, centre pile perforation and insertion/CIP and LW grouting completion/measuring instrument installation
2	08.01-08.24	33	Excavation depth: GL(-)5.1m and 1st-phase strut installation
3	09.01-09.13	22	Excavation depth: GL(-)8.4m and 2nd-phase strut installation
4	10.14-10.31	26	Excavation depth: GL(-)11.0m and 3rd-phase strut installation
5	11.01-11.23	31	Excavation depth: GL(-)13.7m and 4th-phase strut installation
6	12.01-12.31	39	Excavation depth: GL(-)16.5m and 5th-phase strut installation
7	2017.01.01-01.24	33	Excavation depth: GL(-)19.5m and 6th-phase strut installation
8	01.24-01.30	16	Excavation completion: GL(-)25.3m

Table 2 Description of soil deposit

	Thickness	Description	N-Value	Classification
Filled layer	4.0-4.5 m	Gray-brown silty sand-gravel mixture, moist, medium dense	12/30-20/30	SM
Weathered soil	1.2 m	Yellow-brown silty sand, moist, very dense	50/25	SM
Weathered rock	1.3 m	Yellow-brown fragment sand with boring, moist, very dense	50/10	-
Soft rock	15.5-23.5 m	Bedrock, medium or highly weathered, crack and joint, grey-pinkish grey	50/3	-

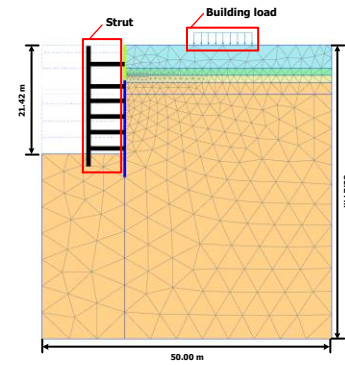
the ground surface (G.L. (-) 0.0 m), and six phases of struts were installed. As seen from the top view and cross-sectional view (Fig. 5 (a) and 5(b), respectively), there were various adjacent structures and roads in use around the site.

The site wall comprised CIP (Cast-In Place Pile) and H-pile and wooden lagging in the upper soil zone and CIP and shotcrete in the lower rock zone; furthermore, the LW grouting method was applied for water cut-off (Fig. 6). After installing piles for the CIP method, excavation was performed, and the struts for each phase were installed for the construction. Table 1 lists details of each construction phase.

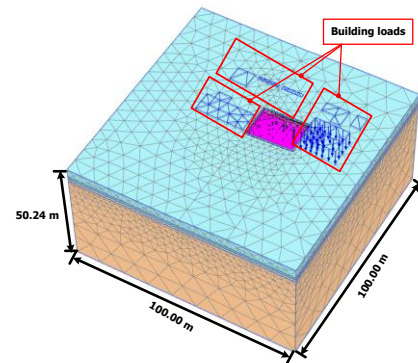
The drilling investigation revealed the type of bedrock, geological structure, and groundwater level. Through a standard penetration test that was conducted simultaneously, the relative density, bearing capacity factor, allowable bearing capacity, adhesion, elastic modulus, softness, and angle of shearing resistance could be estimated. The location of the drilling investigation and the strata sections are shown in Figs. 7(a) and 7(b). The drilling investigation revealed strata in the order of the filled layer, weathered soil, weathered rock, and soft rock (Table 2). The bedrock in the present interval is the banded gneiss, where the mafic mineral part and leucocratic mineral part alternate. The groundwater level was at G.L. (-) 7.7-7.8 m in the soft rock layer.

### 3.2 Back analysis

To assess the field applicability of CPWS, the site at which the existing strut method was applied was modelled through numerical analysis; back analysis was performed first based on the horizontal displacement of the wall, settlement, and axial forces in the struts, as mentioned earlier. Back analysis was performed through two-dimensional (2D) and three-dimensional (3D) numerical



(a) 2D



(b) 3D

Fig. 6 Back analysis modelling for strut method

Table 3 Soil properties

			Filled layer	Weathered soil	Weathered rock	Soft rock
Unit weight	$\gamma_{unsat}$	kN/m <sup>3</sup>	18	19	20	21
Void ratio	$e_{int}$	-	0.5	0.5	0.5	0.5
Young's modulus	E	kN/m <sup>2</sup>	10,898	20,000	45,000	850,000
Poisson's ratio	$\nu$	-	0.35	0.35	0.25	0.25
Cohesion	$c$	kN/m <sup>2</sup>	0	0	10	35
Shear resistance angle	$\phi$	°	23	25	33	35
Dilatancy angle	$\psi$	°	0	0	0	0
Interface	$R_{water}$	-	0.7	0.7	0.7	0.7

Table 4 Wall properties

			CIP	Shotcrete	H-pile
Unit weight	$\gamma$	kN/m <sup>3</sup>	24	24	78.5
Young's modulus	E	MPa	30,000	21,000	21,500
Poisson ratio	$\nu$	-	0.15	0.18	0.2

analysis and by using the commercial software program Plaxis (ver. 2016.02).

The above-mentioned adjacent structures, ground

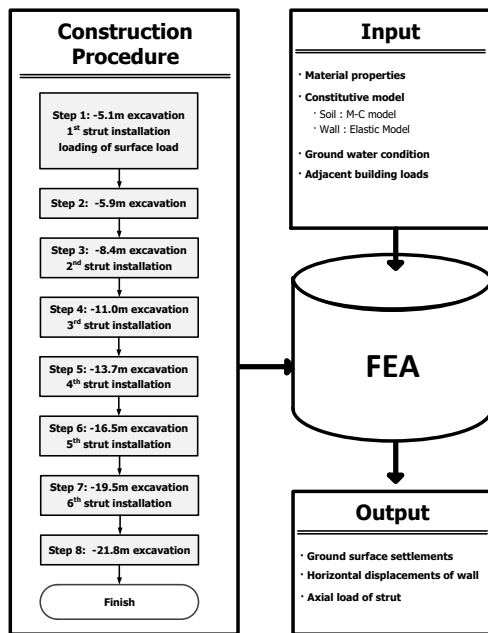


Fig. 7 Procedure of numerical analysis

conditions, groundwater level, and construction phases of the site were modelled. In the case of 2D analysis of a representative section, the horizontal displacement of the wall was measured and the loads of the adjacent structures were estimated according to the conditions of each building.

In 2D and 3D modelling, 1,166 and 198,533 elements were used, respectively (Fig. 6). As for the boundary conditions, the side sections were fixed in the horizontal direction and the bottom surfaces were fixed in all directions.

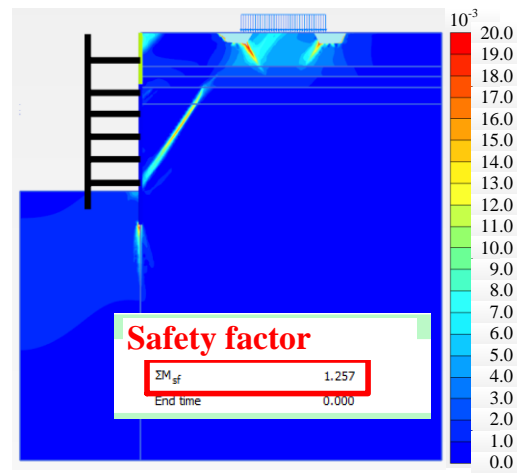
The Mohr-Coulomb constitutive model was used in the numerical analysis; The soil properties were estimated using the N value obtained from the standard penetration test. The physical properties of each structure were referred from the site report and the Korea Geosynthetics Society (2010).

The Plaxis software used in this study represents the interface between the ground and the structure through a strength reduction factor. In Plaxis, the strength reduction factor of the interface between concrete and the ground is generally 0.6-0.7. In this study, a value of 0.7 was obtained in the site measurement. Tables 3 and 4 show the soil properties, strength reduction factor, and wall properties used in the numerical analysis. Fig. 7 shows the overall numerical analysis process.

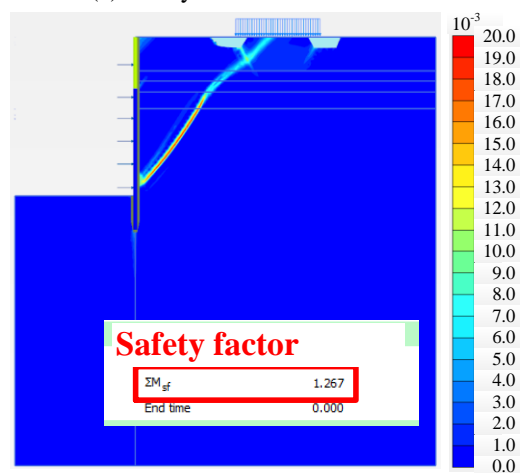
The horizontal displacement of the wall, settlement of the adjacent ground, and axial forces in the struts that were obtained from the site were analysed. The horizontal displacement was measured using an inclinometer; settlement was measured at distances of 1.0, 1.2, and 1.5 m from the wall; and axial forces in the struts were measured in two struts, S1-1 and S2-1 (C), that were installed at the top.

### 3.3 Comparison with field data

The applicability of CPWS in the field can be sorted



(a) Safety factor for strut method



(b) Safety factor for CPWS

Fig. 8 Safety factors from numerical analysis

into the reliability analysis of wall, the displacement of wall and ground, and the safety factor obtained by limit equilibrium analysis. While the reliability analysis of wall can be conducted by using the target reliability index on long-term behaviour through the functions according to corrosion level (Ghasemi and Nowak 2017a, Nowak and Collins 2013, Ghasemi and Nowak 2017b). In this study, however, since the CPWS is a temporary structure which is essential during construction, it has been reviewed by using the only safety factor obtained by limit equilibrium analysis and the displacement of wall and ground. The groundwater level was considered, thus, the safety factor in the rainy season was selected as the baseline. As shown in Fig. 8, the values were respectively 1.26 and 1.27 in strut method and CPWS.

The horizontal displacement of the wall in the final excavation phase and the maximum horizontal displacement depending on the excavation phase are shown in Figs. 9 and 10, respectively. As shown in Fig. 9, the maximum horizontal displacement of the wall in the final excavation phase occurred at the top of the wall. A displacement of 8.38 mm occurred at the top of the wall, and a displacement of -0.10 mm was measured at the final excavation depth of 21 m. The position of each strut installed in each excavation

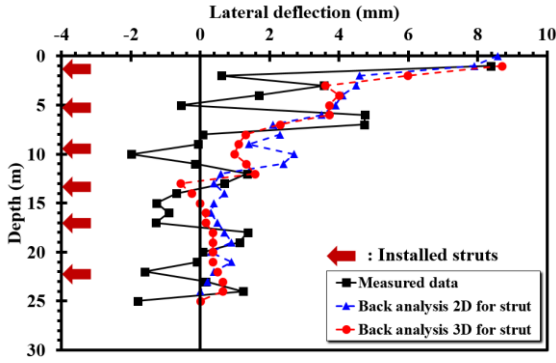


Fig. 9 Lateral deflection for final excavation phase at I-1

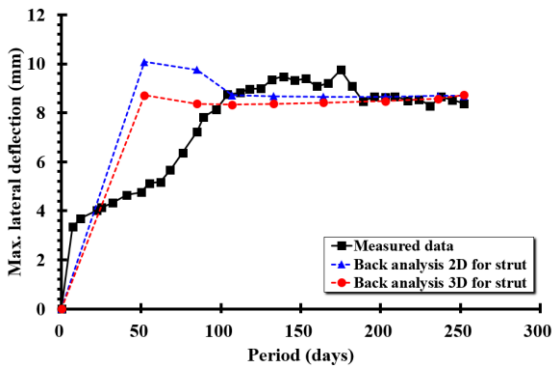


Fig. 10 Maximum lateral deflection depending on construction phase

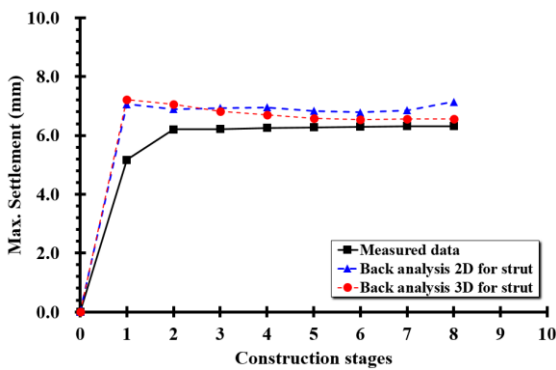


Fig. 11 Maximum settlements depending on construction stages at SE2-1,2,3

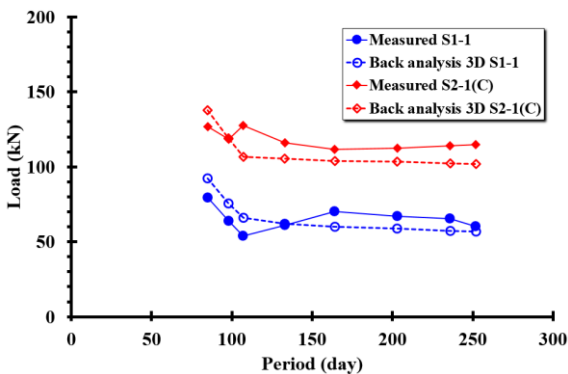
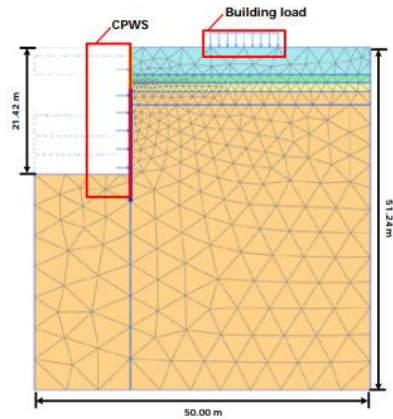
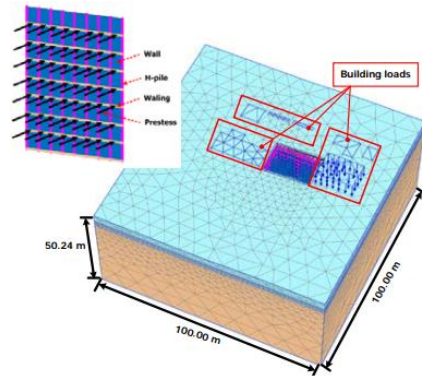


Fig. 12 Load on S1-1 and S2-1(C) struts

phase is indicated by an arrow. It was found that the horizontal displacement of the wall sharply decreased at the



(a) 2D



(b) 3D



(c) Virtual bird's eye view 1



(d) Virtual bird's eye view 2

Fig. 13 Mesh generation and virtual image of CPWS

strut installation positions.

The location where the field-measured value rapidly decreases or becomes negative value shown in Fig. 9 is where the strut is installed. This indicates that the strut influenced the lateral deflection of the wall.

Fig. 10 shows the maximum horizontal displacement of the wall depending on the construction phase. The

maximum horizontal displacement was 9.76 mm in construction phase 5, and then, it gradually converged.

The settlement was measured at SE2-1-3, and the results are shown in Fig. 11. The maximum settlement of 0.32 mm occurred at SE2-1, which was closest to the excavation surface with 0.2 m distance, in the final excavation phase. The next largest settlements of 0.25 and 0.18 mm occurred at SE2-2 and SE2-3, which were 0.7 m and 1.2 m away from the wall, in the final excavation phase, respectively.

The axial forces in S1-1, the main strut, and S2-1(C) installed in the right section were measured using a strain gauge, and the results are shown in Fig. 12. The (+) and (-) signs of the axial force represent compressive and tensile force, respectively. As shown in the figure, both struts were subject to compressive force. The maximum axial force was 79.2 kN in S1-1 and 127.6 kN in S2-1(C), and it was found that 61% larger compressive force occurred in S2-1(C) owing to the stress concentration in the right section.

### 3.4 Modelling for CPWS

To conduct a preliminary analysis of the field applicability of CPWS, CPWS application with the same conditions as for the back analysis of the actual site, where the strut method was applied, was simulated. The prestress was divided into three steps—100, 150, and 200 kN—and gradually increased, and changes in the horizontal displacement of the wall and in the surface settlement were analysed.

Prestress application in CPWS numerical analysis is shown in Fig. 13(a) and 13(b), and the virtual views of the site with CPWS applied are shown in Fig. 13(c) and 13(d). The number of elements formed was 1,188 in 2D and 94,146 in 3D modelling; this was similar to the element number for the back analysis of the strut method.

As for the boundary conditions, the side sections were fixed in the horizontal direction and the bottom surfaces were fixed in all directions as in the case of the back analysis, and the Mohr-Coulomb construction model was used. The soil properties used were the same as those estimated through the back analysis, and the prestress load applied to the wall is shown in Table 5. The tensile force listed in Table 5 was estimated within the allowable range of the  $\phi 12.7$  mm PC strand wire that was used for prestress.

### 3.5 Results from numerical analysis of CPWS

Among the results of 2D and 3D numerical analyses of CPWS, the horizontal displacement of the wall and ground settlement are shown in Figs. 13-15. The maximum horizontal displacement of the wall in the final excavation phase was 7.9 mm near the ground surface (Fig. 14).

Fig. 15 shows the maximum horizontal displacement of the wall depending on the construction phase. The maximum horizontal displacement was  $\sim 8.0$  mm in 2D numerical analysis and 7.0 mm in 3D numerical analysis; however, both 2D and 3D analyses showed similar displacements of  $\sim 8.0$  mm in the final excavation phase. This is a somewhat smaller value compared to the back analysis result of the strut method (8.5 mm).

Fig. 16 shows the settlement according to the excavation

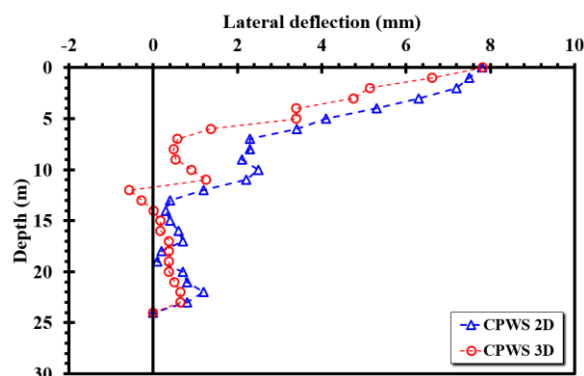


Fig. 14 Lateral deflection depending on depth for CPWS

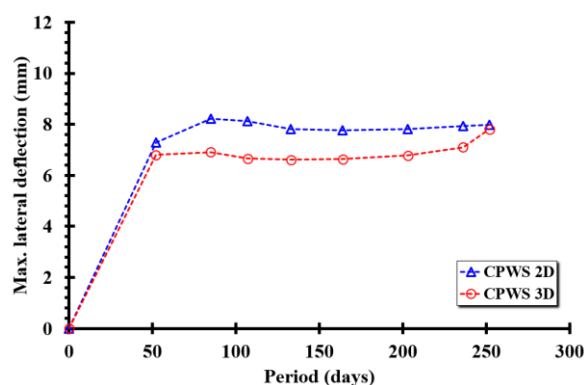


Fig. 15 Maximum lateral deflection depending on construction phase for CPWS

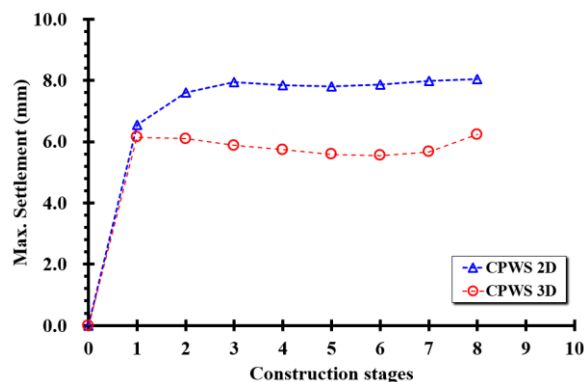


Fig. 16 Settlements at point A for CPWS

phase in the numerical analysis that used CPWS. The settlement predicted using 2D and 3D analysis was 8.0 mm and 6.0 mm, respectively. Although these are somewhat smaller than the values obtained from the site measurement or back analysis result of the strut method, it is believed that the settlement can be reduced further by introducing a larger PC strand wire tension against the earth pressure generated from the back.

## 4. Comparison of results

### 4.1 Results from strut method and CPWS

The field applicability of CPWS was assessed in advance by comparing the site measurement data using the

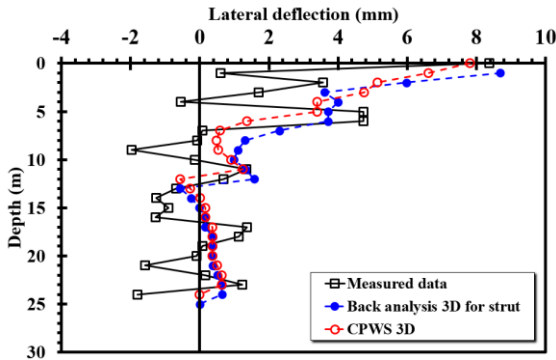


Fig. 17 Comparison of lateral deflection depth

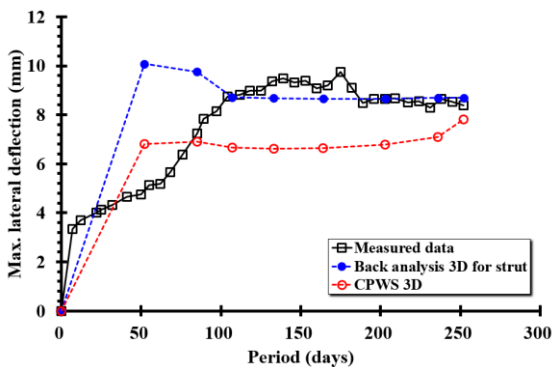


Fig. 18 Comparison of maximum lateral deflection in construction phase

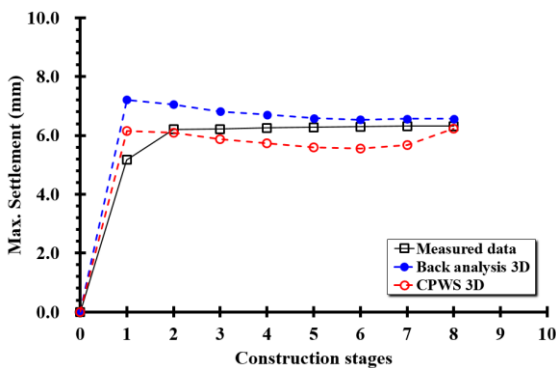


Fig. 19 Maximum settlement in construction phase

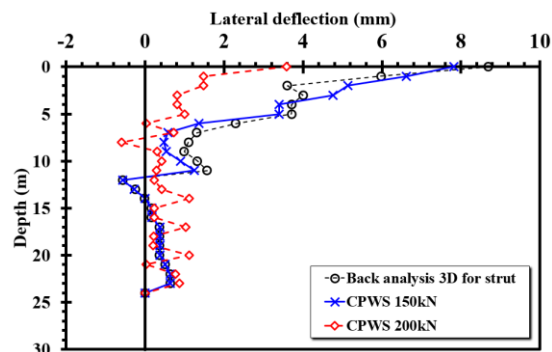


Fig. 20 Lateral deflection according to pre-stress for CPWS

back analysis and numerical analysis of CPWS. Fig. 17 shows the horizontal displacement according to the depth in the final excavation phase. As seen from this figure, all the largest displacements occurred at the top of the wall, and the horizontal displacement of the wall at 7.82 mm in CPWS was 10% smaller than that at 8.69 mm in the back analysis. This was the case when the prestress introduced in the CPWS was 150 kN.

Fig. 18 shows the maximum horizontal displacement of the wall according to the excavation phase. When the results of the back analysis were compared with those of the numerical analysis of CPWS, the largest displacement of the wall occurred at the first-phase excavation and the displacement of the wall gradually converged at later excavation phases. This was somewhat different from the actual measurement results. However, the displacements of the wall in the final excavation phase were 8.0 mm for the site measurement, back analysis, and CPWS numerical analysis.

This means that the application of CPWS does not make much difference compared to the application of the strut method in terms of the horizontal displacement of the wall, that is, structural stability; however, effects such as shortened construction period and improved economic efficiency can be expected by providing sufficient workspace.

The settlements measured at the site were compared with the results of the back analysis and the numerical analysis of CPWS at the same point (Fig. 19). As seen from the figure, the largest settlement change occurred in the 1st phase excavation process for the site measurement, back analysis, and numerical analysis, and the maximum settlements converged to 6.1 mm. As in the case of the above-mentioned maximum horizontal displacement according to the excavation phase, when CPWS is applied in practice, it is believed that the same stability as that achieved using the existing method can be ensured and economic efficiency can be improved by providing sufficient workspace.

#### 4.2 Results from CPWS depending on pre-loading

The CPWS method used in this study has the advantage of being able to adjust the prestress applied to the PC strand wire according to the earth pressure change. Therefore, the horizontal displacement of the wall in the final excavation phase. The prestress was assumed to be 150 and 200 kN, and the same ground and boundary conditions were applied. As seen from Fig. 20, when the prestress was 150 kN, a 7.82 mm horizontal displacement occurred at the top of the wall; this was similar to the value of 8.69 mm obtained from the back analysis result of the strut method. However, when the prestress was increased to 200 kN, a 3.59 mm horizontal displacement occurred; this was 54% lower than the result when the prestress was 150 kN.

### 5. Conclusions

In this study, back analysis was conducted based on measurement data from a site where the strut method was

strut method, back analysis results, and numerical analysis results of CPWS. Only the 3D results were shown for the

applied. In addition, preliminary numerical analysis of the field applicability of the newly developed CPWS method at the same site was conducted by analysing the horizontal displacement of the wall and ground settlement.

- When the horizontal displacement of the wall with depth in the final excavation phase was 10% lower when using the CPWS method than when using the strut method. The maximum horizontal displacement according to the excavation phase was also 23% lower when using the CPWS method than when using the strut method. Therefore, CPWS shows superior field applicability compared to the typical strut method.

- Changes in the horizontal displacement of the wall and in the ground settlement were analysed while the prestress of CPWS was gradually increased. The tension could be applied in the field when compared with the results of the indoor model tests. As a result, when the prestress increased by 33%, the maximum horizontal displacement of the wall and the ground settlement decreased by 54% and 26%, respectively.

- The CPWS, as can be shown in the study results, is not a method for increasing the structural stability by decreasing the horizontal displacement of wall or the settlement of adjacent ground in the prestressed wale system, nor it an typical existing method such as strut. Compared to the existing methods, while wall displacement and settlement occur, a wider work space can be secured, compared to the strut method. Also, unlike the existing prestressed wale system, the tensile force introduced by the PS steel strand can be adjusted and modified according to the changes in the earth pressure during the excavation, which is advantageous.

This shows that CPWS can ensure higher levels of stability against changes in the earth pressure on the wall from the back compared to the existing prestressed wale system. Therefore, CPWS not only affords the advantages of the existing prestressed wale system (i.e., shortened construction period and reduced construction cost by providing sufficient workspace) but also improves the stability against excavation by actively coping with changes in the earth pressure.

## References

- Chowdhury, S.S., Deb, K. and Sengupta, A. (2013), "Estimation of design parameters for braced excavation: Numerical study", *J. Geomech.*, **13**(3), 234-247.
- Civil Engineering and Textile Society (2010), *Reinforced Soil Method*, CIR Publishing, 98.
- Dang, H.P., Lin, H.D., Kung, J.H.S. and Wang, C.C. (2012), "Deformation behavior analyses of braced excavation considering adjacent structure by user-defined soil model", *J. GeoEng.*, **7**(1), 13-20.
- Dong, Y.P., Burd, H.J. and Houlsby, G.T. (2016), "Finite-element analysis of a deep excavation case history", *Geotechnique*, **66**(1), 1-15.
- Dong Y. (2014), "Advanced finite element analysis of deep excavation case histories", Ph.D. Dissertation, University of Oxford, Oxford, U.K.
- Ghasemi, S.H. and Nowak, A.S. (2017a), "Reliability index for non-normal distributions of limit state functions", *Struct. Eng. Mech.*, **62**(3), 365-372.
- Ghasemi, S.H. and Nowak, A.S. (2017b), "Target reliability for bridges with consideration of ultimate limit state", *Eng. Struct.*, **152**, 226-237.
- Huang, X., Huang, H. and Zhang, D. (2012), "Centrifuge modelling of deep excavation over existing tunnel", *Proc. Inst. Civ. Eng. Geotech. Eng.*, **167**(1), 3-18.
- Kim, N.K., Park, J.S., Han, M.Y., Kim, M.Y. and Kim, S.B. (2004), "Development of innovative prestressed support earth retention system", *J. Kor. Geotech. Soc.*, **20**(2), 107-113.
- Kim, M.Y., Lee, J.S., Han, M.Y., Kim, S.B. and Kim, N.K. (2005a), "A multi-noded cable element considering sliding effects", *J. Kor. Soc. Steel Construct.*, **17**(4), 449-457.
- Kim, N.K., Park, J.S., Jang, H.J., Han, M.Y., Kim, M.Y. and Kim, S.B. (2005b), "Performance of innovative prestressed support earth retention system in urban excavation", *J. Kor. Geotech. Soc.*, **21**(2), 27-36.
- Kim, N.K., Park, J.S., Oh, H.J., Han, M.Y., Kim, M.Y. and Kim, S.B. (2007), "Performance of IPS earth retention system in soft clay", *J. Kor. Geotech. Soc.*, **23**(3), 5-13.
- Korea Geosynthetics Society (2010), *Practice of Reinforced Soil Method*, CIR Publishing, 98.
- Kung, G.T.C. (2010), *Finite Element Analysis of Wall Deflection And Ground Movements Caused by Braced Excavations*, in *Finite Element Analysis*, InTech.
- Lee, F.H., Yong, K.Y., Quan, K.C.N. and Chee, K.T. (1998), "Effect of corners in strutted excavations: Field monitoring and case histories", *J. Geotech. Geoenviron. Eng.*, **124**(4), 339-349.
- Leung, R.K., Li, E.S. and Leung, C.L. (2009), "A case study: Design and construction of foundation and braced excavation at a reclaimed site at waterfront", *Proceedings of the State-of-the-art Technology and Experience on Geotechnical Engineering in Malaysia and Hong Kong*, Hong Kong, August.
- Li, D., Li, Z. and Tang, D. (2015), "Three-dimensional effects on deformation of deep excavations", *Proc. Inst. Civ. Eng. Geotech. Eng.*, **168**(6), 551-562.
- Long, M. (2001), "Data for retaining wall and ground movements due to deep excavations", *J. Geotech. Geoenviron. Eng.*, **127**(3), 203-224.
- Nowak, A.S. and Collins, K.R. (2013), *Reliability of Structure*, CRC Press, New York, U.S.A.
- Onishi, K. and Sugawara, T. (1999), "Behavior of an earth retaining wall during deep excavation in Shanghai soft ground", *Soils Found.*, **39**(3), 89-97.
- Osman, A. and Bolton, M. (2007), *Back Analysis of Three Case Histories of Braced Excavations in Boston Blue Clay Using MSD Method*, in *Soft Soil Engineering*, Taylor & Francis, 755-764.
- Osman, A.S. and Bolton, M.D. (2006), "Ground movement predictions for braced excavations undrained clay", *J. Geotech. Geoenviron. Eng.*, **132**(4), 465-477.
- Ou, C.Y., Liao, J.T. and Cheng, W.L. (2000), "Building response and ground movements induced by a deep excavation", *Geotechnique*, **50**(3), 209-220.
- Park, J.S., Joo, Y.S. and Kim, N.K. (2009), "New earth retention system with prestressed wale in urban excavation", *J. Geotech. Geoenviron. Eng.*, **135**(11), 1596-1604.
- Park, J.S., Kim, N.K., Han, M.Y. and Kim, J.W. (2004), "IPS earth retention system", *Proceedings of the Korean Geotechnical Society Spring Conference*, Seoul, Korea, March.
- Pickles, A.R., Lee, S.W. and Norcliffe, B.A.W. (2003), "Groundwater and ground movement around deep excavation", *Proc. Inst. Civ. Eng. Geotech. Eng.*, **156**(3), 147-158.
- Usluogullari, O.F., Temugan, A., Duman, E.S. and Yegin, Y. (2015), "Three dimensional finite element analysis of a deep excavation: Case study in Istanbul Metro", *Proceedings of the*

*16<sup>th</sup> European Conference on Soil Mechanics and Geotechnical Engineering*, Edinburgh, U.K.

Usmani, A., Ramana, G.V. and Sharma, K.G. (2010), "Analysis of braced excavation using hardening soil model", *Proceedings of the Indian Geotechnical Conference*, Mumbai, India, December.

Xu, C., Xu, Y., Sun, H. and Chen, Q. (2013), "Characteristic of braced excavation under asymmetrical loads", *Math. Prob. Eng.*, 1-13.

GC